Applied Physics Letters

Opportunities for nitrogen-vacancy-assisted magnetometry to study magnetism in 2D van der Waals magnets

Cite as: Appl. Phys. Lett. **121**, 060502 (2022); https://doi.org/10.1063/5.0091931
Submitted: 18 March 2022 • Accepted: 21 July 2022 • Published Online: 09 August 2022

Abdelghani Laraoui and Kapildeb Ambal

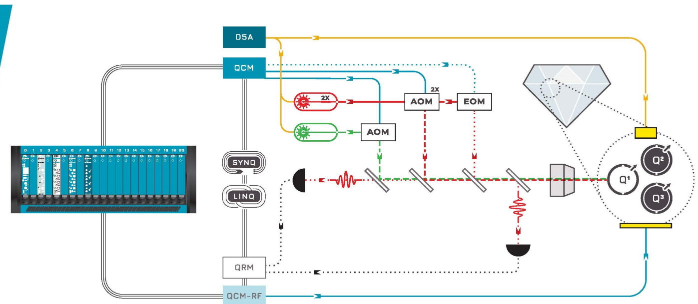

AIP Publishing

Applied Physics Letters PERSPECTIVE scitation.org/journal/apl

Opportunities for nitrogen-vacancy-assisted magnetometry to study magnetism in 2D van der Waals magnets

Cite as: Appl. Phys. Lett. **121**, 060502 (2022); doi: 10.1063/5.0091931
Submitted: 18 March 2022 · Accepted: 21 July 2022 ·
Published Online: 9 August 2022

View Online Export Citation CrossMark

Abdelghani Laraoui[1,a)] and Kapildeb Ambal[2]

AFFILIATIONS

[1]Department of Mechanical and Materials Engineering, University of Nebraska-Lincoln, 900 N 16th St., W342 NH, Lincoln, Nebraska 68588, USA
[2]Department of Mathematics, Statistics, and Physics, Wichita State University, 1845 Fairmount St., Wichita, Kansas 67260, USA

[a)]Author to whom correspondence should be addressed: alaraoui2@unl.edu

ABSTRACT

Exploring and understanding magnetism in two-dimensional (2D) van der Waals (vdW) magnetic materials present a promising route for developing high-speed and low-power spintronics devices. Studying their magnetic properties at the nanoscale is challenging due to their low magnetic moment compared to bulk materials and the requirements of highly sensitive magnetic microscopy tools that work over a wide range of experimental conditions (e.g., temperature, magnetic field, and sample geometry). This Perspective reviews the applications of nitrogen-vacancy center (NV) based magnetometry to study magnetism in 2D vdW magnets. The topics discussed include the basics, advantages, challenges, and the usage of NV magnetometry.

I. OVERVIEW

After the demonstration of the intrinsic magnetic behavior in 2D $Cr_2Ge_2Te_6$ and CrI_3 materials in 2017,[1,2] a wide range of other vdW materials have been investigated.[3] The advantages of 2D magnets in comparison with bulk crystals, such as easy and low-cost fabrication and a wide variety of control mechanisms, make them and their heterostructures promising candidates for the next generation of spintronic devices.[4–7] For example, the extensively studied materials CrI_3 (a semiconductor) and Fe_2GeTe_3 (a metal) are soft ferromagnets in the bulk crystal[8,9] and become hard ferromagnets when exfoliated to a few atomic layers.[10–16] Another advantage of 2D materials is that the atomically thin nature of the material makes it susceptible to adatom engineering and proximity effects.[17,18] By placing graphene on top of a ferromagnetic insulator, anomalous Hall measurements showed that the graphene becomes ferromagnetic.[19,20] Additionally, layer-by-layer engineering and twisting and van der Waals bonding in these materials provide a myriad of magnetic phenomena at the nanoscale, including edge-topological magnetic states,[20] unconventional superconductivity,[21] and topological spin textures such as skyrmions[32] and moiré magnetism.[23] Dopant and defect-induced ferromagnetism has been predicted theoretically[24,25] and demonstrated experimentally in 2D transition metal dichalcogenides (TMD) such as $MoSe_2$, WS_2, MoS_2, VSe_2, and $MnSe_2$.[26–30] This progress has led to the proposal of the usage of 2D magnets in spintronics.[6,7] Examples include the tunneling magnetoresistance devices,[31,32] anomalous Hall effect,[14] spin transistors,[33] spin valves,[34] spin filters and magnetoelectric switches,[16] and magnetic memories based on skyrmions.[22] However, despite this progress, little is known about the mechanisms governing the nanoscale fundamental magnetic processes in 2D vdW magnets.

A wide range of magnetic probing techniques have been used to study their magnetic properties. Standard techniques include magneto-transport measurements,[31,35–39] magneto-optical Kerr effect microscopy (MOKE),[1,2] and magnetic force microscopy (MFM).[40] MOKE is sensitive enough to detect ferromagnetism in few-layer magnets, such as $Cr_2Ge_2Te_6$,[1,2] but it lacks spatial resolution ($\geq$300 nm).[41,42] MFM uses magnetic tips to image the stray magnetic fields generated at surfaces of magnetic materials and has a good spatial resolution $\geq$10 nm, limited by the magnetic tip size and the local magnetic gradient.[43] Apparent contrasts in MFM due to magnetic forces are often contaminated by other long-range forces associated, for instance, with surface charges, that make it hard to interpret the measured magnetic signals quantitatively.[44] MFM also lacks the magnetic sensitivity to image weakly magnetized materials.[44] Advanced microscopy techniques, such as ferromagnetic resonance force microscopy (MRFM),[45] suffer from limited knowledge about the magnetic tip, and magnetic tip influences the local properties. Spin-polarized current-based tunneling microscopy (SP-STM) provides a very good magnetic sensitivity with a spatial resolution of few nanometers,[46,47] but it requires electrically conductive samples. Scanning superconducting quantum interference devices (SQUIDs) integrated to SPM have been used to probe weakly stray-field produced materials, i.e., to measure quantum Hall edge currents in graphene[48] and image orbital ferromagnetism in twisted bilayer graphene.[49] It offers a magnetic sensitivity down to 5 $nT/Hz^{1/2}$ with a spatial resolution below 100 nm, but it needs lower temperatures and complicated SQUID probe designs.[50–52]

Recently, a technique has emerged for measuring magnetic fields at the nanoscale based on optical detection of the electron spin resonances of nitrogen-vacancy (NV) centers in diamond,[53] opening up frontiers to study condensed matter phenomena.[54] NV magnetometry can detect weak static and dynamic magnetic stray fields with frequencies from DC to > few GHz and works at a wide range of experimental conditions, i.e., temperatures from 0.35 to 600 K,[55–58] and applied magnetic fields up to 4 T.[59] It is until very recently where NV magnetometry has been used to study vdW 2D magnets, including CrI_3,[13,23] VI_3,[60] $CrTe_2$,[61] and $CrBr_3$.[62] There are very excellent Review/Perspective papers on studying the magnetic properties of 2D magnets by using various techniques,[4,5,40,63,64] and only a few of them include short discussions of using NV magnetometry.[40] In this Perspective paper, we mainly discuss the advantages and challenges of using NV microscopy to study 2D vdW magnets by including the basics of NV magnetometry sensing/imaging schemes and recent NV-magnetic measurements on 2D magnets, as well as the outlooks of the field.

II. INTRODUCTION TO NV-BASED MAGNETOMETRY SCHEMES

The NV center is a lattice defect in diamond[54,65–67] with remarkable properties, including sensing magnetic fields,[68–75] electrical fields,[76–79] and temperature,[80–82] even at extremes pressure conditions.[83,84] The negatively charged NV center, a substitutional nitrogen adjacent to a vacancy site [Fig. 1(a)], is an $S = 1$ electron spin state that can be initialized by optical excitation (500–550 nm) and detected through spin-dependent photoluminescence (650–800 nm) known as optically detected magnetic resonance (ODMR)[53] [Figs. 1(b) and 1(c)]. Intersystem crossing to metastable singlet states takes place preferentially for NV centers in the $m_s = \pm 1$ states, allowing optical readout of the spin state via spin-dependent fluorescence.[53] The application of a magnetic field breaks the degeneracy of the $m_s = \pm 1$ state via the Zeeman effect and leads to a pair of transitions whose frequencies depend on the magnetic field component along the NV symmetry axis.[53] The NV electron spin has millisecond spin coherence time at room temperature[85–87] and is among the best quantum sensors found in nature.[88] Magnetic field sensing via NV center can be divided into two broad categories based on the spectral characteristics of the magnetic fields to be detected. For example, DC sensing schemes are sensitive to static, slowly varying, and broadband near static magnetic fields, whereas AC sensing schemes typically detect narrowband time-varying magnetic fields of frequency up to few GHz.[54,89,90] NV magnetometry is now widely used to detect static and dynamic magnetic stray fields, temperature, electric field, and strain in solid-state materials, opening up new frontiers in condensed matter research.[54]

The Zeeman shifts of NV's electron spin states are used for DC sensing by measuring the peak positions of NV's spin resonance frequencies.[53] The optimized DC magnetic sensitivity is limited by photon-shot-noise given by Refs. 91–93 as $\eta_{DC} \cong (\gamma_{NV} R)^{-1}\, 1/(I_0 t)]^{1/2}[1/T_2^*]^{1/2}$, where $\gamma_{NV} = 28$ GHz/T is the NV gyromagnetic ratio, R is the ODMR contrast, I_0 is the NV fluorescence rate, T_2^* is the decoherence time of NV, and t is the measurement time. For standard surface NV measurements T_2^* = hundreds of ns to 1.5 μs, giving a DC sensitivity of 4–10 $\mu T/Hz^{1/2}$ for single NVs and < 0.1–1 $\mu T/Hz^{1/2}$ for NV

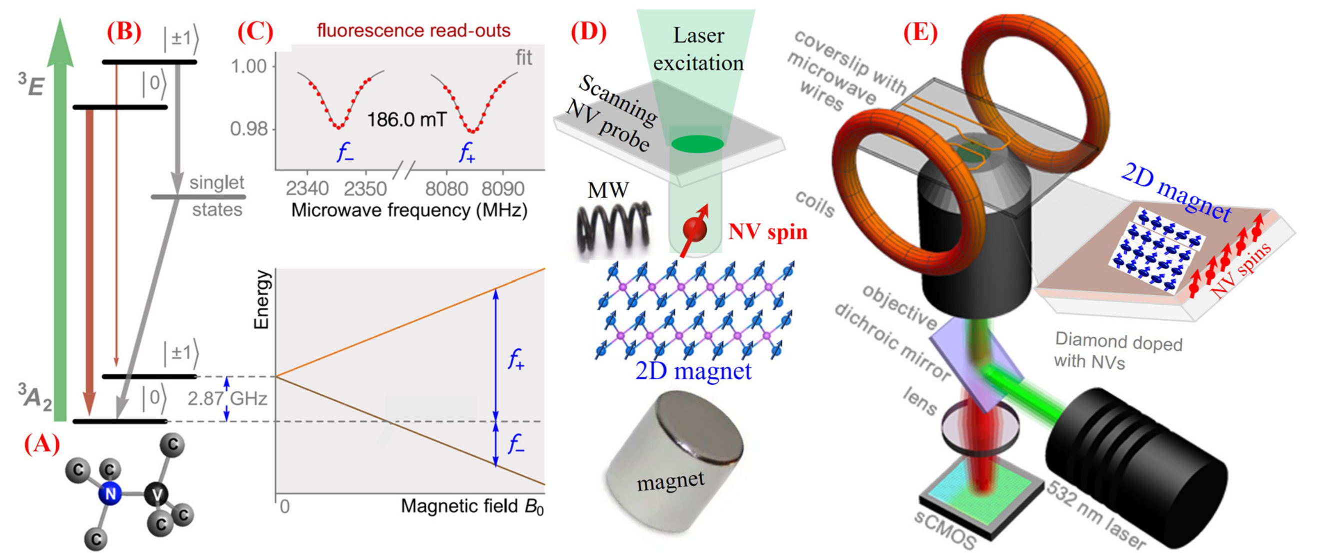

FIG. 1. NV-magnetometry. (a) NV center in the diamond lattice. (b) Energy levels of the NV center. The NV spin is pumped into the $|0\rangle$ state by off resonance optical excitation, and the ground-state spin can be manipulated by microwave excitation. NV ODMR spectra [above (c)] and magnetic field dependence of NV resonances [below (c)]. (d) Schematic of NV-SPM for studying magnetic properties of 2D magnets. (e) Schematic of NV-WFM for studying magnetic properties of 2D magnets. (b) and (c) are reproduced with permission from Fescenko *et al.*, "Diamond magnetic microscopy of malarial hemozoin nanocrystals," Phys. Rev. Appl. **11**, 034029 (2019). Copyright 2021 American Physical Society.[93]

ensembles (densities ~ tens of ppb to few ppm).[91] The variation of the magnetic sensitivities is related to the number of NVs and fluorescence collection efficiency[91] (discussed below). The DC magnetometry scheme is a quick and simple approach to extracting static unknown stray magnetic field B_{NV} (variable magnitude and direction) from magnetic surfaces. Measuring along one of the diamond orientations allows retrieving vector stray field components (B_x, B_y, and B_z) and indirectly retrieving the vector magnetization.[13,54,94]

An AC sensing scheme is preferred to study dynamic magnetic phenomena in 2D magnets,[95] and it offers better magnetic sensitivity and frequency selection as compared to DC sensing protocols.[54,69,96] The NV-magnetometry AC sensing scheme is based on using well-established electron spin resonance pulse sequences such as Hahn echo to extend T_2^* to T_2 (usually one order of magnitude longer).[91] The typical AC magnetic sensitivity for such protocol is about 50–100 nT/Hz$^{1/2}$ for single NVs and can be boosted to few nT/Hz$^{1/2}$ by using pulse dynamical decoupling (DD) protocols and photonics diamond engineering.[91] For example, single NV centers can detect random AC (up to 20 kHz) magnetic fields with a sensitivity of ~50–100 nT/Hz$^{1/2}$ [100]. This AC sensing pulse protocol can be modified to perform double spin resonance experiments and detect high frequency (few GHz) spins.[54,69,70] By using a spin-correlation pulse protocol,[98] the NV AC sensitivity can be pushed down to few nT/Hz$^{1/2}$, limited by the NV spin-lattice relaxation T_1 (few milliseconds at ambient conditions).[91,92,98,99] The spin-correlation pulse protocol is later integrated with DD pulse protocols to probe 30 nuclear ^{11}B spins in atomically thin hBN[100] and map the distribution and direction of the photocurrent flow in the 2D MoS_2 material[90] with sensitivities to current densities as low as 20 nA/μm, comparable to state-of-the-art SQUID.[101] By using NV ensembles in combination with a narrowband synchronized readout protocol,[102,103] AC magnetic sensitivities down to tens of pT/Hz$^{1/2}$ are obtained.[104,105]

III. SCOPE TO DEVELOP FAST, HIGH SPATIAL RESOLUTION, AND HIGHLY SENSITIVE NV MAGNETOMETRY-BASED IMAGING METHODS TO STUDY 2D VDW MAGNETS

There are two approaches for using NV magnetometry for magnetic imaging: single NV scanning probe microscopy [NV-SPM, Fig. 1(d)] and NV ensemble wide-field microscopy [NV-WFM, Fig. 1(e)]. We discuss below in detail the basics of both approaches, advantages, and challenges in comparison with existing magnetic imaging methods.

NV-SPM is proposed first by Degen;[106] NV-SPM is based on scanning a diamond probe with a single NV center across a magnetic sample and measures the stray fields generated from its surface [Fig. 1(d)]. Magnetic imaging with NV-SPM was first realized from DC magnetic stray fields generated by Ni nanoelements[68] but has been extended to imaging skyrmions in ferromagnetic multilayers/films,[94,107,108] spin textures in antiferromagnets,[107,109–112] magnetic vortices in high T_c superconductors,[54,113] and moiré superlattices of twisted 2D magnet CrI_3[23] and to probe magnetic dynamic excitations in ferromagnetic materials.[114,115]

NV-SPM has some advantages to probe magnetism at the nanoscale in comparison with exiting techniques because (1) it provides high spatial resolution (~50 nm), limited by the distance of NV center in the diamond probe from the target surface and by the ambient large tip oscillation amplitude and low Q-factor.[13,58,109,116–118] By using ion beam implantation and slow oxidative etching of implanted diamond, NVs can be created as shallow as 2 nm from the diamond surface.[118] Integrating NV-SPM with an ultra-high vacuum system enhances the diamond tip Q-factor by orders of magnitude, which allow for a lower tip oscillation amplitude.[119] By using these two approaches, the NV-SPM spatial resolution can be pushed down to below 20 nm; (2) commercial diamond tips are available with a single NV center at all diamond orientations that allows measuring samples with different magnetization configurations (e.g., out-of-plane and in-plane); (3) measurements work for both conductive and non-conductive samples, i.e., no surface treatment is required; (4) NV center weakly interacts with the sample, thus, less perturbation, in contrast to MFM; and (5) high sensitivity to static and dynamic magnetic properties[91] (discussed above).

NV-SPM is a still evolving magnetic imaging technique that can be generalized as a standard tool if the challenges discussed below are taken care of. First, it is a slow imaging technique. A typical static magnetic image of 100 × 100 pixels^2 (a dwell time of ~ few seconds per pixel) takes several hours to complete. This is mainly limited by three factors: A long averaging time (tens to hundreds of ms) is required to get a good signal-to-noise ratio, a high number (>20) of MW frequency sweeping points across the ODMR spectrum (linewidth ~5–10 MHz) is needed to resolve weak (<10 μT) stray magnetic fields, and data fitting is used to determine the local magnetic field information per pixel.[13,40,54] There are recent efforts to speed up NV-SPM. Recently, Ambal and McMichael demonstrated a lock-in amplifier detection scheme by using a proportional–integral–derivative (PID) feedback controller to track the NV's ODMR peak with a dwell time of 0.1–1 s.[120,121] However, this method fails to track sudden changes in the local magnetic field.[120] To circumvent this issue, Dushenko *et al.*[122] used an optimized Bayesian algorithm and demonstrated 45 faster acquisition time in comparison with the traditional frequency sweep technique. In this method, the Bayesian algorithm predicts the next best frequency to measure based on previous measurements by learning from each measurement[123] as opposed to the sequentially (step-by-step) frequency sweep. Very recently, Welter *et al.* used a spectrum demodulation method and imaged stray fields above antiferromagnet α-Fe_2O_3 at pixel rates of up to 100 Hz (dwell time = 0.01 s) with an image resolution exceeding one megapixel.[124] This technique is specifically useful for magnetic samples with a large signal dynamic range (~ few mT).[124]

Another approach used to speed up NV-SPM imaging is to optimize the NV's fluorescence collection efficiency in the diamond probe. Placement of the NV center in the diamond probe based on nanopillar geometry boosts the NV fluorescence in comparison with bulk substrates.[125] Hedrich *et al.* fabricated diamond probes with a truncated parabolic profile and optimized the fluorescence signal from single and near-surface NV centers to ~2.1 Mc/s,[126] one order of magnitude better than conventional nanopillar tips (~200 Kc/s).[117] Therefore, combining the parabolic profile of the diamond tip with PID-based tracking or mathematical analysis (e.g., Bayesian algorithm) and spectrum demodulation methods could cut down the NV-SPM imaging time from few tens of seconds to few tens of minutes.

Other challenges of NV-SPM include (i) the requirement of optical and microwave excitation that sometimes sets up a limit on the possible materials to be studied. Laser can excite direct-bandgap 2D magnets and may induce fluorescence in the NV wavelength detection bandwidth.[24,127] Microwave can excite thermal magnon modes in the material and may lead to NV fluorescence quenching and or ODMR broadening.[128,129] It is possible to reduce these effects by using pulsed AC sensing detection schemes;[54,91] (ii) the requirement to align the applied magnetic field along the NV axis to prevent spin level mixing,[53] which leads to a decrease in the NV ODMR contrast and, therefore, deteriorates the NV-SPM sensitivity; and (iii) cryogenic measurements are affected by the reduced photoluminescence contrast, explained by the strain-dependent variations of the NV's orbital g factor.[56] Very recently, NV-SPM imaging has been performed at a temperature of 350 mK,[130] providing opportunities to study high correlated magnetic phenomena in 2D vdW magnets.

NV-WFM: NV-SPM imaging is preferred to map high spatial resolution and small sample regions ($\leq$100 μm^2) with magnetic structures below 100 nm. With NV-ODMR peak tracking techniques and diamond probe engineering (discussed above) could speed up NV-SPM imaging. Though it still may take extra hours to acquire mega-pixel images or scan bigger regions (area >400 μm^2).[13] NV-WFM has emerged as an alternative technique to spatially map solid-state materials and biomolecules.[57] The imaging modality is based on using a diamond chip implanted with a dense layer of NV centers (few nanometers to tens of micrometers) near its surface, interrogated in a wide-field optical microscope with an sCMOS camera, to map the magnetic stray field, lattice strain, temperature, and current density of samples or devices placed in proximity[57] [Fig. 1(e)]. The high density of NVs (a few ppm) allows a DC magnetic sensitivity <0.1 μT/Hz$^{1/2}$ and AC magnetic sensitivity down to tens of pT/Hz$^{1/2}$, depending on the detection volume.[57,91,97] It is used initially to map biomaterials, such as live cells labeled with magnetic nanoparticles[131] and malarial biocrystals[93] and later extended to study magnetism of rocks,[132] and to map local strain in diamonds.[133,134] NV-WFM imaging modality is well suited for rapid analysis (few tens of minutes) of multiple micrometer-sized samples (scanning area >400 μm^2) and allows to study of condensed matter (strain, temperature, and magnetism) phenomena in vdW magnets with sub-300 nm spatial resolution.[57] Measuring the ODMR peaks from the four NV orientations enables vector magnetometry,[135] which is useful for reconstructing the vector magnetization/magnetic moment of 2D magnets. Recently, this modality has been used to study 2D vdW materials, for example, to map current density in a graphene ribbon[136] and stray magnetic field map of VI_3 crystals[60] (further discussion below). Compared with other magneto-optical imaging techniques, such as MOKE, NV-WFM imaging features a similar spatial resolution ($\geq$300 nm, limited by optical diffraction) but presents the advantage of being quantitative, enabling the absolute magnetization of individual flakes to be determined.[57] We discuss below few examples of recent contributions of using NV-SPM and NV-WFM magnetometry to study magnetism in 2D vdW magnets.

IV. RECENT CONTRIBUTION OF NV MAGNETOMETRY TO STUDY 2D MAGNETS

Recently, Thiel *et al.* used NV-SPM to quantitatively study the magnetic properties of CrI_3 monolayers and directly image magnetic domains with a spatial resolution of ~50-nm.[13] Figure 2(a) shows NV measured stray-magnetic field B_{NV} image on an area containing bilayer and trilayer CrI_3 in an applied magnetic field of 172.5 mT. The imaging is performed by measuring the NV full ODMR peaks at each pixel (dwell time of 2 s). The stray magnetic fields come mostly from the edges of the trilayer flake, as expected for a largely uniform

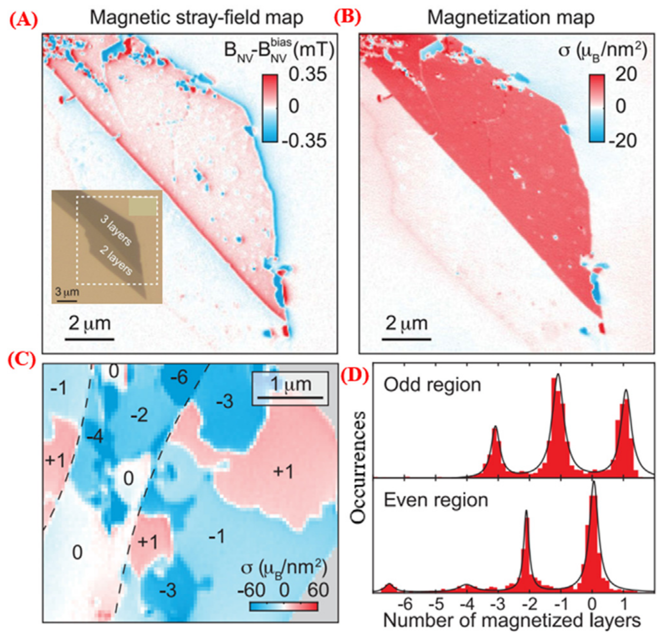

FIG. 2. NV-SPM imaging of CrI_3 layers. (a) NV magnetic stray field map measured at a magnetic field 172. 5 mT, optical image of CrI_3 flake is shown in the inset. (b) Map of the magnetization distribution of the same region, determined by reverse propagation of the NV stray field map in (a). (c) Spontaneously occurring magnetic domains observed in the nine-layer flake of another CrI_3 sample. (d) Histograms of magnetization pixel values obtained in the odd- and even-numbered regions of the data in (c). The figure reproduced with permission from Thiel *et al.*, "Probing magnetism in 2D materials at the nanoscale with single-spin microscopy," Science **364**(6444), 973–976 (2019). Copyright 2019 American Association for the Advancement of Science.[13]

magnetization of few-layer CrI_3.[137] The 2D out-of-plane magnetization map of CrI_3 in Fig. 2(b), retrieved by using a reverse-propagation protocol,[138] shows a uniform magnetization of the trilayer CrI_3 with an average magnetization of ~13 μ_B/nm^2, where μ_B is the Bohr magneton. Additional measurements on different CrI_3 samples with even and odd numbers of layers confirmed the zero net and homogenous magnetization, respectively, consistent with antiferromagnetic exchange coupling.[31,139] The change in the magnetic order from ferromagnet in bulk CrI_3 crystal[11] to antiferromagnetic in CrI_3 layers[10,11,13,139] is explained by the interplay between the structure (stacking order) and exchange coupling.[13] To further explain this effect, NV-SPM measurements were performed on nine-layer flake CrI_3 [Fig. 2(c)]. The spatial variations of the exchange coupling due to the locale change of the stacking order resulted in regions with varying numbers of anti and ferromagnetically coupled layers.[13] The magnetization was found to be discretized in integer multiples of the monolayer magnetization. This domain formation mechanism conserves the parity of well-separated regions on the sample [histogram in Fig. 2(d)] and can be explained by adding or removing a CrI_3 monolayer during sample preparation.[13]

Sun *et al.*[62] employed similar cryogenic NV-SPM to study the existence of magnetic domains in atomically thin $CrBr_3$. $CrBr_3$ is a ferromagnetic insulator with a unique spin system to study ferromagnetism in the 2D limit.[140] The authors studied magnetic domains in few-layer samples of $CrBr_3$ by quantitatively mapping the stray magnetic field.[62] They showed that domain wall pinning is the dominant coercivity mechanism by observing the evolution of both the individual magnetic domains and the average magnetization under variable applied magnetic fields.[62] Song *et al.* used NV-SPM to study the magnetism of twisted layers of the 2D magnet CrI_3 and imaged the magnetic domains in both twisted monolayer and twisted trilayer structures.[23] For twisted trilayers, a periodic moiré pattern of ferromagnetic and antiferromagnetic domains was shown.[141] In a recent NV-SPM study, Fabre *et al.* observed room-temperature ferromagnetism with in-plane magnetic anisotropy in microsized $CrTe_2$ flakes (thickness ~20 nm).[61] The analysis of NV-SPM measurements indicated that the orientation of the magnetization of these flakes is not determined only by shape anisotropy, which suggests the presence of magnetocrystalline anisotropy.[61]

NV-WFM was employed recently by Broadway *et al.* to directly study the magnetic processes in few-layer flakes of VI_3.[60] VI_3 is a magnetic semiconductor that has a hard ferromagnetic behavior in bulk substrates with an out-of-plane anisotropy and a high coercive field H_c of 1 T at low temperatures.[142,143] An optical image of a VI_3 sample on a Si substrate [Fig. 3(a)], prior to transfer to diamond, shows flakes of different thicknesses from three atomic layers up to 10 nm. The NV magnetic field (B_{NV}) image of the same sample, after transfer to diamond [Fig. 3(b)], revealed magnetic signals of up to 50 μT at an applied magnetic field of 5 mT and at a temperature of 5 K. Using a similar approach in reference,[13] the map of the out-of-plane magnetization (M_z) is reconstructed in Fig. 3(c) and found to be in the range of ~50 μ_B/nm^2. A complete and abrupt switching of most flakes is observed at coercive field $H_c \approx$ 0.5–1 T, independent of VI_3 flake thickness, as shown in Fig. 3(d). H_c decreases as the temperature approaches the Curie temperature T_c ($\approx$50 K). To understand the switching processes in the VI_3 flakes, 1 s pulses of magnetic field are applied in the -z-direction of the samples (initially magnetized in the +z-direction) and the NV-ODMR imaging is performed by increasing the magnetic field pulse amplitude up to 1.3 T and temperature up to 50 K. The magnetization was found to reverse abruptly, and H_c decreases with the increase in temperature [Fig. 3(e)]. This observation has a similar signature of magnetic domain nucleation-type as in ferromagnetic systems.[144] Further NV-WFM measurements from the zero-field cooled state to high magnetic fields up to 0.4 T and at 5 K are performed on the same flake. The domain wall depinning field in the range of 0.1 T to 0.4 T increases with the decrease in the flake thickness.[60] These values, expected from thin flakes, are way less in the case of bulk crystals (~ few mT) measured by MOKE.[143]

These demonstrations of using NV magnetometry in both NV-SPM and NV-WFM are promising, paving the way toward the widespread use of this technique as a powerful microscopy tool to study magnetism in 2D vdW magnets.

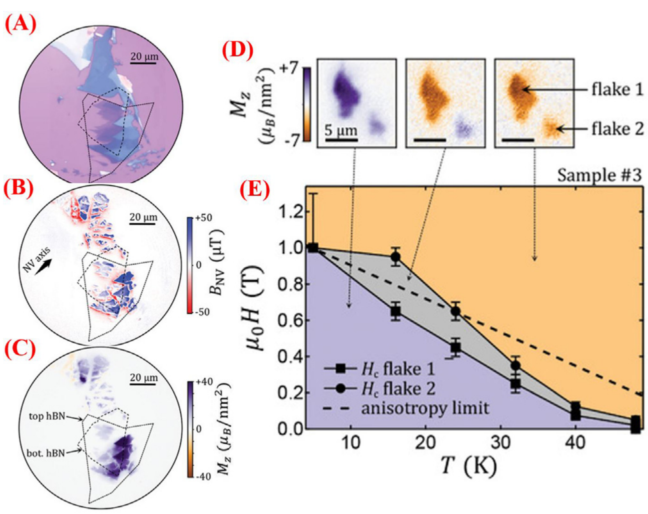

FIG. 3. NV-WFM imaging of few-layer VI_3 flakes. (a) Optical image of VI3 flake with varying thickness prior to transfer to the diamond. (b) The corresponding NV B_{NV} map at 5 K and bias magnetic field of 5 mT. (c) Map of z magnetization Mz determined from (b). (d) Mz maps of each magnetic state in (e), recorded at 5 K. (e) H–T phase diagram of the magnetic state of two flakes. The figure is reproduced with permission from Broadway *et al.*, "Imaging domain reversal in an ultrathin van der Waals ferromagnet," Adv. Mater. **32**, 2003314 (2020). Copyright 1999–2021 John Wiley & Sons, Inc.[60]

V SUMMARY AND FUTURE PERSPECTIVE

NV magnetometry is still an emerging technique with impressive progress over the last few years. We highlighted some of the progress toward a wide usage of such techniques: The commercialization of single NV diamond probes with different orientations that allow measuring 2D magnets with any magnetization orientation; the commercialization of turn-key RT and cryogenic NV-SPM microscopes may expand the usage to non-NV experts, the demonstration of 350 mK NV-SPM operation may provide opportunities to study high correlated magnetic phenomena in 2D magnets;[55] the integration of lock-in detection, Bayesian approach, or demodulation methods can speed up the acquisition time of NV-SPM.[122–124] The usage of NV-WFM can help in rapid analysis of multiple micrometer-sized samples and allow for studying condensed matter (strain, transport, temperature, and magnetism) phenomena in vdW magnets.[57]

In comparison with standard magnetic imaging techniques, NV magnetometry has several advantages summarized here: its high sensitivity to surface magnetic samples,[13,40,58,109] detection of dynamic magnetic excitation,[37,69,145] and sensitivity to other parameters, such as electric field, local strain, and temperature, that make it an ideal hybrid quantum sensing platform for 2D magnets. However, the requirements of magnetic field alignment, laser, and high-frequency MW excitation, and short (few nanometers) NV-to-target sample distance[58,128] add few limitations to NV magnetometry. By complementing NV magnetometry with magneto-transport measurements and with other magnetic probing techniques, it can be an ideal tool to study spin textures, spin dynamics and relaxation, and the origin of magnetism in 2D vdW magnets. For example, there are many recent studies where NV magnetometry (both NV-SPM and NV-WFM) is integrated with magneto-transport measurements to study current-induced nanoscale fragmentation of non-uniform antiferromagnetic domain patterns in CuMnAs devices[146] and study spin–orbit torque induced deterministic magnetic switching and chiral spin rotation in non-collinear antiferromagnet Mn_3Sn,[147] opening a new door to study antiferromagnetism in 2D magnets.

ACKNOWLEDGMENTS

A.L. would like to acknowledge the support of the National Science Foundation/EPSCoR RII Track-1: Emergent Quantum Materials and Technologies (EQUATE), Award No. OIA-2044049.

The research was performed, in part, in the Nebraska Nanoscale Facility: National Nanotechnology Coordinated Infrastructure and the Nebraska Center for Materials and Nanoscience (and/or NERCF), which are supported by the National Science Foundation under Award No. ECCS: 2025298, and the Nebraska Research Initiative. K.A. would like to acknowledge the support of the National Science Foundation/EPSCoR RII Track-4 Award No. OIA-2033210 and the Wichita State University Convergence Science Initiative Program.

AUTHOR DECLARATIONS

Conflict of Interest

The authors have no conflicts to disclose.

Author Contributions

Abdelghani Laraoui: Conceptualization (equal); Writing – original draft (equal); Writing – review and editing (equal). **Kapildeb Ambal:** Conceptualization (equal); Writing – original draft (equal); Writing – review and editing (equal).

DATA AVAILABILITY

Data sharing is not applicable to this article as no new data were created or analyzed in this study.

REFERENCES

[1] C. Gong, L. Li, Z. Li *et al.*, "Discovery of intrinsic ferromagnetism in two-dimensional van der Waals crystals," Nature **546**, 265 (2017).

[2] B. Huang, G. Clark, E. Navarro-Moratalla *et al.*, "Layer-dependent ferromagnetism in a van der Waals crystal down to the monolayer limit," Nature **546**, 270 (2017).

[3] C. Gong and X. Zhang, "Two-dimensional magnetic crystals and emergent heterostructure devices," Science **363**, eaav4450 (2019).

[4] W. Zhang, P. K. J. Wong, R. Zhu, and A. T. S. Wee, "Van der Waals magnets: Wonder building blocks for two-dimensional spintronics?," InfoMat **1**, 479 (2019).

[5] V. P. Ningrum, B. Liu, W. Wang *et al.*, "Recent advances in two-dimensional magnets: Physics and devices towards spintronic applications," Res. **2020**, 1768918.

[6] G. Hu and B. Xiang, "Recent advances in two-dimensional spintronics," Nanoscale Res. Lett. **15**, 226 (2020).

[7] Y. Liu, C. Zeng, J. Zhong, J. Ding, Z. M. Wang, and Z. Liu, "Spintronics in two-dimensional materials," Nano-Micro Lett. **12**, 93 (2020).

[8] X. Zhang, Y. Zhao, Q. Song, S. Jia, J. Shi, and W. Han, "Magnetic anisotropy of the single-crystalline ferromagnetic insulator $Cr_2Ge_2Te_6$," Jpn. J. Appl. Phys. **55**, 033001 (2016).

[9] B. Chen, J. Yang, H. Wang, M. Imai, H. Ohta, C. Michioka, K. Yoshimura, and M. Fang, "Magnetic properties of layered itinerant electron ferromagnet Fe_3GeTe_2," J. Phys. Soc. Jpn. **82**, 124711 (2013).

[10] B. Huang, G. Clark, D. R. Klein *et al.*, "Electrical control of 2D magnetism in bilayer CrI_3," Nat. Nanotechnol. **13**, 544 (2018).

[11] J. Kim, K.-W. Kim, B. Kim, C.-J. Kang, D. Shin, S.-H. Lee, B.-C. Min, and N. Park, "Exploitable magnetic anisotropy of the two-dimensional magnet CrI_3," Nano Lett. **20**, 929 (2020).

[12] W. Jina, Z. Yeb, and X. Luo *et al.*, "Tunable layered-magnetism–assisted magneto-Raman effect in a two-dimensional magnet CrI_3," Proc. Natl. Acad. Sci. **117**, 24664 (2020).

[13] L. Thiel, Z. Wang, M. A. Tschudin, D. Rohner, I. Gutiérrez-Lezama, N. Ubrig, M. Gibertini, E. Giannini, A. F. Morpurgo, and P. Maletinsky, "Probing magnetism in 2D materials at the nanoscale with single-spin microscopy," Science **364**(6444), 973–976 (2019).

[14] C. Tan, J. Lee, S.-G. Jung, T. Park, S. Albarakati, J. Partridge, M. R. Field, D. G. McCulloch, L. Wang, and C. Lee, "Hard magnetic properties in nanoflake van der Waals Fe_3GeTe_2," Nat. Commun. **9**, 1554 (2018).

[15] R. Roemer, C. Liu, and K. Zou, "Robust ferromagnetism in wafer-scale monolayer and multilayer Fe_3GeTe_2," npj 2D Mater. Appl. **4**(1), 33 (2020).

[16] X. Wang, J. Tang, X. Xia *et al.*, "Current-driven magnetization switching in a van der Waals ferromagnet Fe_3GeTe_2," Sci. Adv. **5**, eaaw8904 (2019).

[17] K. M. McCreary, A. G. Swartz, W. Han, J. Fabian, and R. K. Kawakami, "Magnetic moment formation in graphene detected by scattering of pure spin currents," Phys. Rev. Lett. **109**, 186604 (2012).

[18] X. Hong, K. Zou, B. Wang, S.-H. Cheng, and J. Zhu, "Evidence for spin-flip scattering and local moments in dilute fluorinated graphene," Phys. Rev. Lett. **108**, 226602 (2012).

[19] Z. Wang, C. Tang, R. Sachs, Y. Barlas, and J. Shi, "Proximity-induced ferromagnetism in graphene revealed by the anomalous Hall effect," Phys. Rev. Lett. **114**, 016603 (2015).

[20] J. C. Leutenantsmeyer, A. A. Kaverzin, M. Wojtaszek, and B. J. van Wees, "Proximity induced room temperature ferromagnetism in graphene probed with spin currents," 2D Mater. **4**, 014001 (2016).

[21] D. Shen, C. N. Kuo, T. W. Yang, I. N. Chen, C. S. Lue, and L. M. Wang, "Two-dimensional superconductivity and magnetotransport from topological surface states in $AuSn_4$ semimetal," Commun. Mater. **1**(1), 56 (2020).

[22] Y. Wu, S. Zhang, J. Zhang *et al.*, "Néel-type skyrmion in WTe_2/Fe_3GeTe_2 van der Waals heterostructure," Nat. Commun. **11**, 3860 (2020).

[23] T. Song, Q.-C. Sun, E. Anderson *et al.*, "Direct visualization of magnetic domains and moiré magnetism in twisted 2D magnets," Science **374**, 1140 (2021).

[24] X.-L. Fan, Y.-R. An, and W.-J. Guo, "Ferromagnetism in transitional metal-doped MoS_2 monolayer," Nanoscale Res. Lett. **11**, 154 (2016).

[25] M. R. Habib, W. Chen, W.-Y. Yin, H. Su, and M. Xu, "Simulation of transition metal dichalcogenides," in *Two Dimensional Transition Metal Dichalcogenides: Synthesis, Properties, and Applications*, edited by N. S. Arul and V. D. Nithya (Springer, Singapore, 2019), pp. 135–172.

[26] L. Cai, J. He, Q. Liu *et al.*, "Vacancy-induced ferromagnetism of MoS_2 nanosheets," J. Am. Chem. Soc. **137**, 2622 (2015).

[27] F. Zhang, B. Zheng, A. Sebastian *et al.*, "Monolayer vanadium-doped tungsten disulfide: A room-temperature dilute magnetic semiconductor," Adv. Sci. **7**, 2001174 (2020).

[28] S. Fu, K. Kang, K. Shayan *et al.*, "Enabling room temperature ferromagnetism in monolayer MoS_2 via in situ iron-doping," Nat. Commun. **11**, 2034 (2020).

[29] W. Yu, J. Li, T. S. Herng *et al.*, "Chemically exfoliated VSe_2 monolayers with room-temperature ferromagnetism," Adv. Mater. **31**, 1903779 (2019).

[30] D. J. O'Hara, T. Zhu, A. H. Trout *et al.*, "Room temperature intrinsic ferromagnetism in epitaxial manganese selenide films in the monolayer limit," Nano Lett. **18**, 3125 (2018).

[31] T. Song, X. Cai, M. W.-Y. Tu *et al.*, "Giant tunneling magnetoresistance in spin-filter van der Waals heterostructures," Science **360**, 1214 (2018).

[32] L. Meng, Z. Zhou, M. Xu *et al.*, "Anomalous thickness dependence of curie temperature in air-stable two-dimensional ferromagnetic 1T-$CrTe_2$ grown by chemical vapor deposition," Nat. Commun. **12**, 809 (2021).

[33] S. Jiang, L. Li, Z. Wang, J. Shan, and K. F. Mak, "Spin tunnel field-effect transistors based on two-dimensional van der Waals heterostructures," Nat. Electron. **2**, 159 (2019).

[34] Z. Wang, D. Sapkota, T. Taniguchi, K. Watanabe, D. Mandrus, and A. F. Morpurgo, "Tunneling spin valves based on Fe_3GeTe_2/HBN/Fe_3GeTe_2 van der Waals heterostructures," Nano Lett. **18**, 4303 (2018).

[35] J. Yan, X. Luo, F. C. Chen *et al.*, "Anomalous Hall effect in two-dimensional non-collinear antiferromagnetic semiconductor $Cr_{0.68}Se$," Appl. Phys. Lett. **111**, 022401 (2017).

[36] Y. Wang, C. Xian, J. Wang, B. Liu, L. Ling, L. Zhang, L. Cao, Z. Qu, and Y. Xiong, "Anisotropic anomalous Hall effect in triangular itinerant ferromagnet Fe_3GeTe_2," Phys. Rev. B **96**, 134428 (2017).

[37] W. Xing, L. Qiu, X. Wang, Y. Yao, Y. Ma, R. Cai, S. Jia, X. C. Xie, and W. Han, "Magnon transport in quasi-two-dimensional van der Waals antiferromagnets," Phys. Rev. X **9**, 011026 (2019).

[38] Z. Wang, T. Zhang, M. Ding *et al.*, "Electric-field control of magnetism in a few-layered van der Waals ferromagnetic semiconductor," Nat. Nanotechnol. **13**, 554 (2018).

[39]Z. Wang, I. Gutiérrez-Lezama, N. Ubrig, M. Kroner, M. Gibertini, T. Taniguchi, K. Watanabe, A. Imamoğlu, E. Giannini, and A. F. Morpurgo, "Very large tunneling magnetoresistance in layered magnetic semiconductor CrI_3," Nat. Commun. **9**, 2516 (2018).

[40]E. Marchiori, L. Ceccarelli, N. Rossi, L. Lorenzelli, C. L. Degen, and M. Poggio, "Nanoscale magnetic field imaging for 2D materials," Nat. Rev. Phys. **4**, 49 (2022).

[41]A. Laraoui, M. Vomir, J. Vénuat, M. Albrecht, E. Beaurepaire, and J.-Y. Bigot, "Time resolved magneto-optical microscopy of individual ferromagnetic dots," in *15th International Conference on Ultrafast Phenomena* (Optica Publishing Group, 2006), p. TuD6.

[42]A. Laraoui, M. Albrecht, and J.-Y. Bigot, "Femtosecond magneto-optical Kerr microscopy," Opt. Lett. **32**, 936 (2007).

[43]R. Nagatsu, M. Ohtake, M. Futamoto, F. Kirino, and N. Inaba, "Spatial resolution and switching field of magnetic force microscope tips prepared by coating Fe/Co-Pt layers," AIP Adv. **6**, 056503 (2016).

[44]S.-W. Cheong, M. Fiebig, W. Wu, L. Chapon, and V. Kiryukhin, "Seeing is believing: Visualization of antiferromagnetic domains," npj Quantum Mater. **5**, 3 (2020).

[45]C. L. Degen, M. Poggio, H. J. Mamin, C. T. Rettner, and D. Rugar, "Nanoscale magnetic resonance imaging," Proc. Natl. Acad. Sci. **106**, 1313 (2009).

[46]R. Wiesendanger, "Spin mapping at the nanoscale and atomic scale," Rev. Mod. Phys. **81**, 1495 (2009).

[47]A. Schlenhoff, S. Kovarik, S. Krause, and R. Wiesendanger, "Real-space imaging of atomic-scale spin textures at nanometer distances," Appl. Phys. Lett. **116**, 122406 (2020).

[48]A. Uri, Y. Kim, K. Bagani *et al.*, "Nanoscale imaging of equilibrium quantum Hall edge currents and of the magnetic monopole response in graphene," Nat. Phys. **16**, 164 (2020).

[49]C. L. Tschirhart, M. Serlin, H. Polshyn *et al.*, "Imaging orbital ferromagnetism in a moiré Chern insulator," Science **372**, 1323 (2021).

[50]A. Finkler, D. Vasyukov, Y. Segev *et al.*, "Nano-sized SQUID-on-tip for scanning probe microscopy," J. Phys.: Conf. Ser. **400**, 052004 (2012).

[51]D. Vasyukov, Y. Anahory, L. Embon *et al.*, "A scanning superconducting quantum interference device with single electron spin sensitivity," Nat. Nanotechnol. **8**, 639 (2013).

[52]Y. Anahory, L. Embon, C. J. Li *et al.*, "Emergent nanoscale superparamagnetism at oxide interfaces," Nat. Commun. **7**, 12566 (2016).

[53]M. W. Doherty, N. B. Manson, P. Delaney, F. Jelezko, J. Wrachtrup, and L. C. L. Hollenberg, "The nitrogen-vacancy colour centre in diamond," Phys. Rep. **528**(1), 1–45 (2013).

[54]F. Casola, T. van der Sar, and A. Yacoby, "Probing condensed matter physics with magnetometry based on nitrogen-vacancy centres in diamond," Nat. Rev. Mater. **3**(1), 17088 (2018).

[55]P. J. Scheidegger, S. Diesch, M. L. Palm, and C. L. Degen, "Scanning nitrogen-vacancy magnetometry down to 350 MK," Appl. Phys. Lett. **120**, 224001 (2022).

[56]J. Happacher, D. Broadway, P. Reiser *et al.*, "Low-temperature photophysics of single nitrogen-vacancy centers in diamond," Phys. Rev. Lett. **128**, 177401 (2022).

[57]S. C. Scholten, A. J. Healey, I. O. Robertson, G. J. Abrahams, D. A. Broadway, and J.-P. Tetienne, "Widefield quantum microscopy with nitrogen-vacancy centers in diamond: Strengths, limitations, and prospects," J. Appl. Phys. **130**, 150902 (2021).

[58]P. Maletinsky, S. Hong, M. S. Grinolds, B. Hausmann, M. D. Lukin, R. L. Walsworth, M. Loncar, and A. Yacoby, "A robust scanning diamond sensor for nanoscale imaging with single nitrogen-vacancy centres," Nat. Nanotechnol. **7**, 320 (2012).

[59]B. Fortman and S. Takahashi, "Understanding the linewidth of the ESR spectrum detected by a single NV center in diamond," J. Phys. Chem. A **123**, 6350 (2019).

[60]D. A. Broadway, S. C. Scholten, C. Tan *et al.*, "Imaging domain reversal in an ultrathin van der Waals ferromagnet," Adv. Mater. **32**, 2003314 (2020).

[61]F. Fabre, A. Finco, A. Purbawati, A. Hadj-Azzem, N. Rougemaille, J. Coraux, I. Philip, and V. Jacques, "Characterization of room-temperature in-plane magnetization in thin flakes of $CrTe_2$ with a single-spin magnetometer," Phys. Rev. Mater. **5**, 034008 (2021).

[62]Q.-C. Sun, T. Song, E. Anderson *et al.*, "Magnetic domains and domain wall pinning in atomically thin $CrBr_3$ revealed by nanoscale imaging," Nat. Commun. **12**, 1989 (2021).

[63]Y. L. Huang, W. Chen, and A. T. S. Wee, "Two-dimensional magnetic transition metal chalcogenides," SmartMat **2**, 139 (2021).

[64]S. Kumari, D. K. Pradhan, N. R. Pradhan, and P. D. Rack, "Recent developments on 2D magnetic materials: Challenges and opportunities," Emergent Mater. **4**, 827 (2021).

[65]H. J. Mamin, M. Kim, M. H. Sherwood, C. T. Rettner, K. Ohno, D. D. Awschalom, and D. Rugar, "Nanoscale nuclear magnetic resonance with a nitrogen-vacancy spin sensor," Science **339**, 557 (2013).

[66]A. Gruber, A. Dräbenstedt, C. Tietz, L. Fleury, J. Wrachtrup, and C. v Borczyskowski, "Scanning confocal optical microscopy and magnetic resonance on single defect centers," Science **276**, 2012 (1997).

[67]R. Schirhagl, K. Chang, M. Loretz, and C. L. Degen, "Nitrogen-vacancy centers in diamond: Nanoscale sensors for physics and biology," Annu. Rev. Phys. Chem. **65**, 83 (2014).

[68]G. Balasubramanian, I. Y. Chan, R. Kolesov *et al.*, "Nanoscale imaging magnetometry with diamond spins under ambient conditions," Nature **455**, 648 (2008).

[69]T. van der Sar, F. Casola, R. Walsworth, and A. Yacoby, "Nanometre-scale probing of spin waves using single electron spins," Nat. Commun. **6**, 7886 (2015).

[70]A. Laraoui, J. S. Hodges, and C. A. Meriles, "Nitrogen-vacancy-assisted magnetometry of paramagnetic centers in an individual diamond nanocrystal," Nano Lett. **12**, 3477 (2012).

[71]A. Laraoui and C. A. Meriles, "Approach to dark spin cooling in a diamond nanocrystal," ACS Nano **7**, 3403 (2013).

[72]H. Clevenson, L. M. Pham, C. Teale, K. Johnson, D. Englund, and D. Braje, "Robust high-dynamic-range vector magnetometry with nitrogen-vacancy centers in diamond," Appl. Phys. Lett. **112**, 252406 (2018).

[73]T. Wolf, P. Neumann, K. Nakamura, H. Sumiya, T. Ohshima, J. Isoya, and J. Wrachtrup, "Subpicotesla diamond magnetometry," Phys. Rev. X **5**, 041001 (2015).

[74]D. Paone, D. Pinto, G. Kim *et al.*, "All-optical and microwave-free detection of Meissner screening using nitrogen-vacancy centers in diamond," J. Appl. Phys. **129**, 024306 (2021).

[75]D. Pinto, D. Paone, B. Kern *et al.*, "Readout and control of an endofullerene electronic spin," Nat. Commun. **11**, 6405 (2020).

[76]F. Dolde, H. Fedder, M. W. Doherty *et al.*, "Electric-field sensing using single diamond spins," Nat. Phys. **7**, 459 (2011).

[77]M. S. J. Barson, L. M. Oberg, L. P. McGuinness, A. Denisenko, N. B. Manson, J. Wrachtrup, and M. W. Doherty, "Nanoscale vector electric field imaging using a single electron spin," Nano Lett. **21**, 2962 (2021).

[78]M. Block, B. Kobrin, A. Jarmola *et al.*, "Optically enhanced electric field sensing using nitrogen-vacancy ensembles," Phys. Rev. Appl. **16**, 024024 (2021).

[79]J. Michl, J. Steiner, A. Denisenko *et al.*, "Robust and accurate electric field sensing with solid state spin ensembles," Nano Lett. **19**, 4904 (2019).

[80]A. Laraoui, H. Aycock-Rizzo, Y. Gao, X. Lu, E. Riedo, and C. A. Meriles, "Imaging thermal conductivity with nanoscale resolution using a scanning spin probe," Nat. Commun. **6**, 8954 (2015).

[81]G. Kucsko, P. C. Maurer, N. Y. Yao, M. Kubo, H. J. Noh, P. K. Lo, H. Park, and M. D. Lukin, "Nanometre-scale thermometry in a living cell," Nature **500**, 54 (2013).

[82]V. M. Acosta, E. Bauch, M. P. Ledbetter, A. Waxman, L.-S. Bouchard, and D. Budker, "Temperature dependence of the nitrogen-vacancy magnetic resonance in diamond," Phys. Rev. Lett. **104**, 070801 (2010).

[83]M. Lesik, T. Plisson, L. Toraille *et al.*, "Magnetic measurements on micrometer-sized samples under high pressure using designed NV centers," Science **366**(6471), 1359–1313 (2019).

[84]M. W. Doherty, V. V. Struzhkin, D. A. Simpson *et al.*, "Electronic properties and metrology applications of the diamond NV center under pressure," Phys. Rev. Lett. **112**, 047601 (2014).

[85]G. Balasubramanian, P. Neumann, D. Twitchen *et al.*, "Ultralong spin coherence time in isotopically engineered diamond," Nat. Mater. **8**, 383 (2009).

[86]N. Bar-Gill, L. M. Pham, A. Jarmola, D. Budker, and R. L. Walsworth, "Solid-state electronic spin coherence time approaching one second," Nat. Commun. **4**, 1743 (2013).
[87]E. D. Herbschleb, H. Kato, Y. Maruyama *et al.*, "Ultra-long coherence times amongst room-temperature solid-state spins," Nat. Commun. **10**, 3766 (2019).
[88]C. L. Degen, F. Reinhard, and P. Cappellaro, "Quantum sensing," Rev. Mod. Phys. **89**, 035002 (2017).
[89]G. Wang, Y.-X. Liu, J. M. Schloss, S. T. Alsid, D. A. Braje, and P. Cappellaro, "Sensing of arbitrary-frequency fields using a quantum mixer," Phys. Rev. X **12**, 021061 (2022).
[90]B. B. Zhou, P. C. Jerger, K.-H. Lee, M. Fukami, F. Mujid, J. Park, and D. D. Awschalom, "Spatiotemporal mapping of a photocurrent vortex in monolayer MoS_2 using diamond quantum sensors," Phys. Rev. X **10**, 011003 (2020).
[91]J. F. Barry, J. M. Schloss, E. Bauch, M. J. Turner, C. A. Hart, L. M. Pham, and R. L. Walsworth, "Sensitivity optimization for NV-diamond magnetometry," Rev. Mod. Phys. **92**, 015004 (2020).
[92]J. R. Maze, P. L. Stanwix, J. S. Hodges *et al.*, "Nanoscale magnetic sensing with an individual electronic spin in diamond," Nature **455**, 644 (2008).
[93]I. Fescenko, A. Laraoui, J. Smits, N. Mosavian, P. Kehayias, J. Seto, L. Bougas, A. Jarmola, and V. M. Acosta, "Diamond magnetic microscopy of malarial hemozoin nanocrystals," Phys. Rev. Appl. **11**, 034029 (2019).
[94]Y. Dovzhenko, F. Casola, S. Schlotter, T. X. Zhou, F. Büttner, R. L. Walsworth, G. S. D. Beach, and A. Yacoby, "Magnetostatic twists in room-temperature skyrmions explored by nitrogen-vacancy center spin texture reconstruction," Nat. Commun. **9**, 2712 (2018).
[95]M. Gibertini, M. Koperski, A. F. Morpurgo, and K. S. Novoselov, "Magnetic 2D materials and heterostructures," Nat. Nanotechnol. **14**, 408 (2019).
[96]C. Du, T. Van der Sar, T. X. Zhou *et al.*, "Control and local measurement of the spin chemical potential in a magnetic insulator," Science **357**, 195–198 (2017).
[97]A. Laraoui, J. S. Hodges, and C. A. Meriles, "Magnetometry of random ac magnetic fields using a single nitrogen-vacancy center," Appl. Phys. Lett. **97**, 143104 (2010).
[98]A. Laraoui, F. Dolde, C. Burk, F. Reinhard, J. Wrachtrup, and C. A. Meriles, "High-resolution correlation spectroscopy of 13C spins near a nitrogen-vacancy centre in diamond," Nat. Commun. **4**, 1651 (2013).
[99]P. Kehayias, A. Jarmola, N. Mosavian *et al.*, "Solution nuclear magnetic resonance spectroscopy on a nanostructured diamond chip," Nat. Commun. **8**, 188 (2017).
[100]I. Lovchinsky, J. D. Sanchez-Yamagishi, E. K. Urbach *et al.*, "Magnetic resonance spectroscopy of an atomically thin material using a single-spin qubit," Science **355**(6324), 503–507 (2017).
[101]Y. Anahory, J. Reiner, L. Embon, D. Halbertal, A. Yakovenko, Y. Myasoedov, M. L. Rappaport, M. E. Huber, and E. Zeldov, "Three-junction SQUID-on-tip with tunable in-plane and out-of-plane magnetic field sensitivity," Nano Lett. **14**, 6481 (2014).
[102]S. Schmitt, T. Gefen, F. M. Stürner *et al.*, "Submillihertz magnetic spectroscopy performed with a nanoscale quantum sensor," Science **356**(6340), 832–837 (2017).
[103]J. M. Boss, K. S. Cujia, J. Zopes, and C. L. Degen, "Quantum sensing with arbitrary frequency resolution," Science **356**(6340), 837–840 (2017).
[104]D. R. Glenn, D. B. Bucher, J. Lee, M. D. Lukin, H. Park, and R. L. Walsworth, "High-resolution magnetic resonance spectroscopy using a solid-state spin sensor," Nature **555**, 351 (2018).
[105]J. Smits, J. T. Damron, P. Kehayias, A. F. McDowell, N. Mosavian, I. Fescenko, N. Ristoff, A. Laraoui, A. Jarmola, and V. M. Acosta, "Two-dimensional nuclear magnetic resonance spectroscopy with a microfluidic diamond quantum sensor," Sci. Adv. **5**, eaaw7895 (2019).
[106]C. L. Degen, "Scanning magnetic field microscope with a diamond single-spin sensor," Appl. Phys. Lett. **92**, 243111 (2008).
[107]A. Finco, A. Haykal, R. Tanos *et al.*, "Imaging non-collinear antiferromagnetic textures via single spin relaxometry," Nat. Commun. **12**, 767 (2021).
[108]I. Gross, L. J. Martínez, J.-P. Tetienne *et al.*, "Direct measurement of interfacial Dzyaloshinskii–Moriya interaction in X | CoFeB | MgO heterostructures with a scanning NV magnetometer (X = Ta, TaN, and W)," Phys. Rev. B **94**, 064413 (2016).
[109]I. Gross, W. Akhtar, V. Garcia *et al.*, "Real-space imaging of non-collinear antiferromagnetic order with a single-spin magnetometer," Nature **549**, 252 (2017).
[110]A. Erickson, A. Mahmood, S. Q. A. Shah, R. Timalsina, C. Binek, and A. Laraoui, "Nansocale imaging of antiferromagnetic domains in epitaxial Cr_2O_3 films using diamond quantum sensing microscopy," in *Bulletin of the American Physical Society* (American Physical Society, 2022).
[111]M. S. Wörnle, P. Welter, M. Giraldo, T. Lottermoser, M. Fiebig, P. Gambardella, and C. L. Degen, "Coexistence of Bloch and Néel walls in a collinear antiferromagnet," Phys. Rev. B **103**, 094426 (2021).
[112]N. Hedrich, K. Wagner, O. V. Pylypovskyi, B. J. Shields, T. Kosub, D. D. Sheka, D. Makarov, and P. Maletinsky, "Nanoscale mechanics of antiferromagnetic domain walls," Nat. Phys. **17**, 574 (2021).
[113]M. Pelliccione, A. Jenkins, P. Ovartchaiyapong, C. Reetz, E. Emmanouilidou, N. Ni, and A. C. Bleszynski Jayich, "Scanned probe imaging of nanoscale magnetism at cryogenic temperatures with a single-spin quantum sensor," Nat. Nanotechnol. **11**, 700 (2016).
[114]T. X. Zhou, J. J. Carmiggelt, L. M. Gächter *et al.*, "A magnon scattering platform," Proc. Natl. Acad. Sci. **118**, e2019473118 (2021).
[115]B. G. Simon, S. Kurdi, H. La, I. Bertelli, J. J. Carmiggelt, M. Ruf, N. de Jong, H. van den Berg, A. J. Katan, and T. van der Sar, "Directional excitation of a high-density magnon gas using coherently driven spin waves," Nano Lett. **21**, 8213 (2021).
[116]L. Thiel, D. Rohner, M. Ganzhorn, P. Appel, E. Neu, B. Müller, R. Kleiner, D. Koelle, and P. Maletinsky, "Quantitative nanoscale vortex imaging using a cryogenic quantum magnetometer," Nat. Nanotechnol. **11**, 677 (2016).
[117]P. Appel, E. Neu, M. Ganzhorn, A. Barfuss, M. Batzer, M. Gratz, A. Tschöpe, and P. Maletinsky, "Fabrication of all diamond scanning probes for nanoscale magnetometry," Rev. Sci. Instrum. **87**, 063703 (2016).
[118]M. Loretz, S. Pezzagna, J. Meijer, and C. L. Degen, "Nanoscale nuclear magnetic resonance with a 1.9-nm-deep nitrogen-vacancy sensor," Appl. Phys. Lett. **104**, 033102 (2014).
[119]T. An, T. Eguchi, K. Akiyama, and Y. Hasegawa, "Atomically-resolved imaging by frequency-modulation atomic force microscopy using a quartz length-extension resonator," Appl. Phys. Lett. **87**, 133114 (2005).
[120]K. Ambal and R. D. McMichael, "A differential rate meter for real-time peak tracking in optically detected magnetic resonance at low photon count rates," Rev. Sci. Instrum. **90**, 023907 (2019).
[121]K. Ambal and R. D. McMichael, "Device method to transform discrete voltage pulses to a phase-sensitive continuous signal," U.S. patent 10999109B2 (4 May 2021).
[122]S. Dushenko, K. Ambal, and R. D. McMichael, "Sequential Bayesian experiment design for optically detected magnetic resonance of nitrogen-vacancy centers," Phys. Rev. Appl. **14**, 054036 (2020).
[123]M. Caouette-Mansour, A. Solyom, B. Ruffolo, R. D. McMichael, J. Sankey, and L. Childress, "Robust spin relaxometry with fast adaptive Bayesian estimation," Phys. Rev. Appl. **17**, 064031 (2022).
[124]P. Welter, B. A. Josteinsson, S. Josephy, A. Wittmann, A. Morales, G. Puebla-Hellmann, and C. L. Degen, "Fast scanning nitrogen-vacancy magnetometry by spectrum demodulation," e-print arXiv:2205.06579 (2022).
[125]T. M. Babinec, B. J. M. Hausmann, M. Khan, Y. Zhang, J. R. Maze, P. R. Hemmer, and M. Lončar, "A diamond nanowire single-photon source," Nat. Nanotechnol. **5**, 195 (2010).
[126]N. Hedrich, D. Rohner, M. Batzer, P. Maletinsky, and B. J. Shields, "Parabolic diamond scanning probes for single-spin magnetic field imaging," Phys. Rev. Appl. **14**, 064007 (2020).
[127]L. Tao, F. Meng, S. Zhao *et al.*, "Experimental and theoretical evidence for the ferromagnetic edge in WSe_2 nanosheets," Nanoscale **9**, 4898 (2017).
[128]T. X. Zhou, R. J. Stöhr, and A. Yacoby, "Scanning diamond NV center probes compatible with conventional AFM technology," Appl. Phys. Lett. **111**, 163106 (2017).
[129]C. S. Wolfe, S. A. Manuilov, C. M. Purser, R. Teeling-Smith, C. Dubs, P. C. Hammel, and V. P. Bhallamudi, "Spatially resolved detection of complex ferromagnetic dynamics using optically detected nitrogen-vacancy spins," Appl. Phys. Lett. **108**, 232409 (2016).
[130]X. Liu, Z. Hao, E. Khalaf *et al.*, "Tunable spin-polarized correlated states in twisted double bilayer graphene," Nature **583**, 221 (2020).

[131]D. L. Sage, K. Arai, D. R. Glenn, S. J. DeVience, L. M. Pham, L. Rahn-Lee, M. D. Lukin, A. Yacoby, A. Komeili, and R. L. Walsworth, "Optical magnetic imaging of living cells," Nature **496**, 486 (2013).

[132]D. R. Glenn, R. R. Fu, P. Kehayias, D. L. Sage, E. A. Lima, B. P. Weiss, and R. L. Walsworth, "Micrometer-scale magnetic imaging of geological samples using a quantum diamond microscope," Geochem. Geophys. Geosyst. **18**, 3254 (2017).

[133]P. Kehayias, M. J. Turner, R. Trubko, J. M. Schloss, C. A. Hart, M. Wesson, D. R. Glenn, and R. L. Walsworth, "Imaging crystal stress in diamond using ensembles of nitrogen-vacancy centers," Phys. Rev. B **100**, 174103 (2019).

[134]D. A. Broadway, B. C. Johnson, M. S. J. Barson *et al.*, "Microscopic imaging of the stress tensor in diamond using in situ quantum sensors," Nano Lett. **19**, 4543 (2019).

[135]B. J. Maertz, A. P. Wijnheijmer, G. D. Fuchs, M. E. Nowakowski, and D. D. Awschalom, "Vector magnetic field microscopy using nitrogen vacancy centers in diamond," Appl. Phys. Lett. **96**, 092504 (2010).

[136]J.-P. Tetienne, N. Dontschuk, D. A. Broadway, A. Stacey, D. A. Simpson, and L. C. L. Hollenberg, "Quantum Imaging of current flow in graphene," Sci. Adv. **3**(4), e1602429 (2017).

[137]T. Hingant, J.-P. Tetienne, L. J. Martínez, K. Garcia, D. Ravelosona, J.-F. Roch, and V. Jacques, "Measuring the magnetic moment density in patterned ultra-thin ferromagnets with submicrometer resolution," Phys. Rev. Appl. **4**, 014003 (2015).

[138]B. J. Roth, N. G. Sepulveda, and J. P. Wikswo, "Using a magnetometer to image a two-dimensional current distribution," J. Appl. Phys. **65**, 361 (1989).

[139]S. Jiang, L. Li, Z. Wang, K. F. Mak, and J. Shan, "Controlling magnetism in 2D CrI_3 by electrostatic doping," Nat. Nanotechnol. **13**, 549 (2018).

[140]H. H. Kim, B. Yang, S. Li *et al.*, "Evolution of interlayer and intralayer magnetism in three atomically thin chromium trihalides," Proc. Natl. Acad. Sci. **116**, 11131 (2019).

[141]Z. Qiu, M. Holwill, T. Olsen, P. Lyu, J. Li, H. Fang, H. Yang, M. Kashchenko, K. S. Novoselov, and J. Lu, "Visualizing atomic structure and magnetism of 2D magnetic insulators via tunneling through graphene," Nat. Commun. **12**, 70 (2021).

[142]S. Tian, J.-F. Zhang, C. Li, T. Ying, S. Li, X. Zhang, K. Liu, and H. Lei, "Ferromagnetic van der Waals crystal VI_3," J. Am. Chem. Soc. **141**, 5326 (2019).

[143]T. Kong, K. Stolze, E. I. Timmons, J. Tao, D. Ni, S. Guo, Z. Yang, R. Prozorov, and R. J. Cava, "VI_3—A new layered ferromagnetic semiconductor," Adv. Mater. **31**, 1808074 (2019).

[144]A. Laraoui, J. Vénuat, V. Halté, M. Albrecht, E. Beaurepaire, and J.-Y. Bigot, "Study of individual ferromagnetic disks with femtosecond optical pulses," J. Appl. Phys. **101**, 09C105 (2007).

[145]Z. Zhang, J. Shang, C. Jiang, A. Rasmita, W. Gao, and T. Yu, "Direct photoluminescence probing of ferromagnetism in monolayer two-dimensional $CrBr_3$," Nano Lett. **19**, 3138 (2019).

[146]M. S. Wörnle, P. Welter, Z. Kašpar, K. Olejník, V. Novák, R. P. Campion, P. Wadley, T. Jungwirth, C. L. Degen, and P. Gambardella, "Current-induced fragmentation of antiferromagnetic domains," e-print arXiv:1912.05287 (2019).

[147]G. Q. Yan, S. Li, H. Lu *et al.*, "Quantum sensing and imaging of spin–orbit-torque-driven spin dynamics in the non-collinear antiferromagnet Mn_3Sn," Adv. Mater. **34**, 2200327 (2022).